TABLE V

MANTISSAS AND EXPONENT PRE/POST PROCESSING COMPLEXITY OF COMPLEX BLOCK ALU

Block Addition	**Mantissas Scaling**	**Exponents Arithmetic**
Complex IEEE754	$4*N$	$2*N$
Common Exponent	$4*N$	2
Exponent Box	$8*N$	4
Block Multiplication	**Mantissas Scaling**	**Exponents Arithmetic**
Complex IEEE754	$8*N$	$6*N$
Common Exponent	$8*N$	2
Exponent Box	$16*N$	5
Convolution	**Mantissas Scaling**	**Exponents Arithmetic**
Complex IEEE754	$6*N_1N_2+4*(N_1-1)(N_2-1)$	$6*N_1N_2+2*(N_1-1)(N_2-1)$
Common Exponent	$6*N_1N_2+4*(N_1-1)(N_2-1)$	$3*(N_1+N_2-1)+1$
Exponent Box	$10*N_1N_2+8*(N_1-1)(N_2-1)$	$3*(N_1+N_2-1)+1$

of the complex block output. With Exponent Box Encoding in the worst case, we need eight more mantissas post-scaling. Also, the Shift Vectors allow for four possible intermediate exponent values instead of one intermediate exponent value in Common Exponent Encoding.

C. Complex Convolution

Let $\boldsymbol{X_1} \in \mathbb{C}^{1\times N_1}$, $\boldsymbol{X_2} \in \mathbb{C}^{1\times N_2}$, and $\boldsymbol{Y} \in \mathbb{C}^{1\times(N_1+N_2-1)}$ be complex-valued row vectors, where $*$ denotes convolution, such that,

$$\begin{aligned}\Re\{\boldsymbol{Y}\} &= \Re\{\boldsymbol{X_1} * \boldsymbol{X_2}\}\\ \Im\{\boldsymbol{Y}\} &= \Im\{\boldsymbol{X_1} * \boldsymbol{X_2}\}\end{aligned} \tag{3}$$

We assume $N_1 < N_2$ for practical reason where the model of channel impulse response has shorter sequence than the discrete-time samples. Each term in the complex block output is complex inner product of two complex block input of varying length between 1 and $min\{N_1, N_2\}$. Complex convolution is implemented as complex block multiplication and accumulation of intermediate results. We derive the processing complexity of mantissas and exponents in Appendix .

IV. SYSTEM MODEL

We apply Exponent Box Encoding to represent IQ components in baseband QAM transmitter in Figure 5 and baseband QAM receiver in Figure 6. The simulated channel model is Additive White Gaussian Noise (AWGN). Table VI contains the parameter definitions and values used in MATLAB simulation and Table VII summarizes the memory input/output rates (bits/sec) and multiply-accumulate rates required by discrete-time complex QAM transmitter and receiver chains.

A. Discrete-time Complex Baseband QAM Transmitter

We encode complex block IQ samples in Exponent Box Encoding and retain the floating-point resolution in 32-bit IEEE-754 precision in our model. For simplicity, we select block size to be, $N_v = L^{TX} f_{sym}$. The symbol mapper generates a $L^{TX} f_{sym}$-size of complex block IQ samples that shares common exponent. Pulse shape filter is implemented as Finite Impulse Response (FIR) filter of N^{TX}-order and requires complex convolution on the upsampled complex block IQ samples.

TABLE VI

QAM TRANSMITTER, RECEIVER SPECIFICATIONS

QAM Parameters	Definition	Values / Types
Constellation Order	M	1024
Transceiver Parameters	Definition	Values / Types
Up-sample Factor	L^{TX}, L^{RX}	4
Symbol Rate (Hz)	f_{sym}	2400
Filter Order	N^{TX}, N^{RX}	32^{th}
Pulse Shape	g^{TX}, g^{RX}	Root-Raised Cosine
Excess Bandwidth Factor	α^{Tx}, α^{RX}	0.2

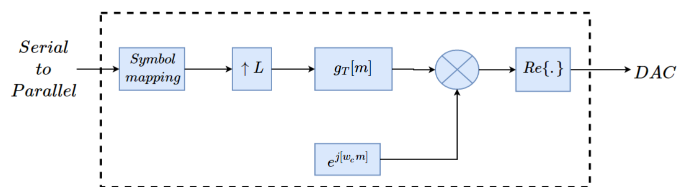

Fig. 5. Block diagram of discrete-time complex baseband QAM transmitter

B. Discrete-time Complex Baseband QAM Receiver

Due to the channel effect such as fading in practice, the received signals will have larger span in magnitude-phase response. The Common Exponent Encoding applied on sampled complex block IQ samples is limited to selecting window size of minimum phase difference. The Common Exponent Encoding must update its block size at the update rate of gain by the Automatic Gain Control (AGC). Instead, our Exponent Box Encoding could lift the constraint and selects fixed block size, $N_v = L^{RX} f_{sym}$ in this simulation. We simulate matched filter of N^{RX}-order.

V. SIMULATION RESULTS

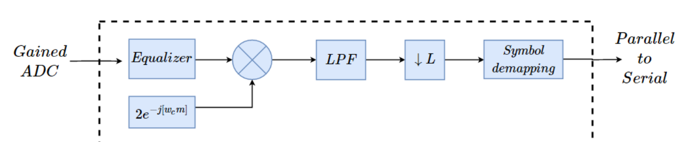

Fig. 6. Block diagram of discrete-time complex baseband QAM receiver